



# OPEN Three-dimensional agitated saline contrast transesophageal echocardiography for the diagnosis of patent foramen ovale

Seo-Yeon Gwak, Kyu Kim, Hyun-Jung Lee, Iksung Cho, Geu-Ru Hong, Jong-Won Ha & Chi Young Shim✉

Patent foramen ovale (PFO) is a three-dimensional (3D) and dynamic structure, making diagnosis challenging with 2D imaging. We aimed to develop a practical 3D agitated saline contrast (ASC) transesophageal echocardiography (TEE) protocol, assess its feasibility, and evaluate its diagnostic implications in ischemic stroke patients. In 158 ischemic stroke patients (52 women; age:  $63.6 \pm 14.0$  years) undergoing TEE to assess embolic sources, 2D and 3D ASC tests were performed using the EPIQ CVx ultrasound system (Philips Medical Systems, Andover, MA) with a 2–8 MHz transesophageal matrix array transducer (X8-2t). Patients were categorized into four groups: no shunt, possible PFO, definite PFO, and intrapulmonary shunt. The practical 3D ASC protocol included bicaval ( $90^\circ$ – $120^\circ$ ) and short-axis ( $40^\circ$ – $70^\circ$ ) views at the mid-esophageal level, visualizing the left upper pulmonary vein and interatrial septum. Image acquisition was feasible in 150 patients (94.9%). By applying the 3D ASC protocol, 32 patients (21.3%) were reclassified into another group. Definite PFO cases increased from 20 (13.3%) to 35 (23.3%). The 3D ASC TEE protocol is feasible and improves the accuracy of PFO diagnosis in ischemic stroke patients, offering added value over 2D TEE.

**Keywords** Three-dimensional, Agitated saline contrast, Transesophageal echocardiography, Patent foramen ovale

## Abbreviations

ASA	Atrial septal aneurysm
ASC	Agitated saline contrast
IPS	Intrapulmonary shunt
LA	Left atrium
PFO	Patent foramen ovale
TEE	Transesophageal echocardiography
TTE	Transthoracic echocardiography

Patent foramen ovale (PFO) has been known to cause cryptogenic stroke and recurrent ischemic stroke in various clinical situations<sup>1–3</sup>. Therefore, it is clinically important to accurately diagnose PFO and evaluate its functional grade and structure to appropriately select patients who require PFO closure and prevent recurrent stroke<sup>4–6</sup>. An agitated saline contrast (ASC) study based on 2D transesophageal echocardiography (TEE) has been used as the gold standard for PFO diagnosis<sup>7–9</sup>. In the real world, TEE is particularly useful in evaluating PFO anatomy in patients with cryptogenic stroke and suspected PFO<sup>10</sup>. However, because the 2D image only shows one plane in the 3D space, it has limited accuracy in identifying the PFO opening and often makes it challenging to capture air bubbles entering the left atrium (LA). In addition, the differential diagnosis of PFO from extracardiac shunt remains challenging in clinical practice even if the three-to-five-beat rule is applied<sup>8,11,12</sup>. This is because capturing the atrial septum and pulmonary vein on a single screen in 2D images is difficult; therefore, verifying the path and 3D direction of the air bubble movement is challenging. Consequently, ambiguous cases can be misdiagnosed as false-positive or false-negative PFO in the ASC test<sup>13</sup>.

Three-dimensional image acquisition during TEE has become common in various clinical situations due to recent advances in 3D TEE techniques<sup>14–16</sup>. Some efforts have been made to utilize 3D TEE for the detection and

Division of Cardiology, Severance Cardiovascular Hospital, Yonsei University College of Medicine, 50–1 Yonsei-ro, Seodaemun-gu, Seoul 03722, Republic of Korea. ✉email: cysprs@yuhs.ac

structural evaluation of PFO<sup>17,18</sup>. Theoretically, 3D TEE can visualize the entire PFO anatomy and surrounding structures and is likely to show high certainty in differentiating intracardiac shunt from extracardiac shunt<sup>18</sup>. However, in real clinical practice, poor image quality during the Valsalva maneuver, the requirement of recording 3D images for at least ten beats after relieving the Valsalva maneuver, and patient discomfort during the additional acquisition time for 3D images are major barriers to the application of 3D techniques in evaluating the cause of paradoxical right-to-left shunt. Considering that the spatial and temporal resolutions of 3D TEE have improved remarkably, we speculated that 3D TEE could be of practical use for PFO diagnosis and intrapulmonary shunt (IPS) discrimination if a protocol that minimizes the necessity of additional images is applied. Therefore, we attempted to develop a practical protocol to detect PFO using 3D TEE, evaluate its feasibility, and explore the advantages and incremental value of 3D TEE compared to 2D TEE in detecting PFO in patients with ischemic stroke.

## Methods

### Study population

We enrolled 158 patients with ischemic stroke who underwent TEE between April 2021 and January 2023 at Severance Cardiovascular Hospital, Seoul, Korea, for the evaluation of the cardiac source of embolism. Ischemic stroke was confirmed by a focal neurological deficit with sudden onset and by magnetic resonance imaging findings. Patients' clinical information was obtained at the time of TEE. National Institutes of Health Stroke Scale (NIHSS) scores and stroke etiology were investigated. The etiologies were classified into three categories: embolic stroke of undetermined source (ESUS), atherosclerosis, and lacunar infarction<sup>19</sup>. A total of 150 patients were included in the final analysis after excluding eight patients with unsuitable images because of inappropriate Valsalva maneuvers or poor image quality. An inappropriate Valsalva maneuver was defined as the absence of leftward bulging of the interatrial septum during the release phase and/or inadequate opacification of the right atrial septal region<sup>20</sup>. Poor image quality was defined as insufficient visualization of the interatrial septum during the Valsalva maneuver. The study was approved by the Institutional Review Board of Yonsei University Health System (IRB number: 4-2023-0318) and was conducted in accordance with the Declaration of Helsinki. Informed consent was waived for this study as approved by the Institutional Review Board of Yonsei University Health System in accordance with applicable guidelines and regulations.

### Diagnosis of PFO using 2D and 3D TEE

TEE was performed using the EPIQ CVx ultrasound system (Philips Medical Systems, Andover, MA, USA), equipped with a 2–8 MHz transesophageal matrix array transducer (X8-2t), which offers the benefits of faster data processing, improved image quality, and tailored examination tools. Standard 2D assessments were performed as recommended by the American Society of Echocardiography<sup>21</sup>. The Valsalva maneuver was performed after the initial agitated saline injection at rest, following the acquisition of standard TEE views. Agitated saline was prepared using  $\geq 8$  mL of preservative-free normal saline and 0.5–1 mL of room air, vigorously agitated between two syringes connected by a three-way stopcock, following ASE guideline recommendations<sup>22</sup>. Up to three agitated saline injections were allowed for each of the 2D and 3D assessments (maximum of six total), depending on image quality and the adequacy of the Valsalva maneuver. All patients were fully conscious during the examination and performed the Valsalva maneuver actively under verbal instruction. The same examiner acquired the 3D dataset of the PFO immediately after the standard 2D assessment, using a second injection of agitated saline. As 2D and 3D imaging cannot be performed simultaneously, a separate acquisition was required. However, all injections followed a standardized protocol with consistent Valsalva guidance to minimize variability.

Based on the 2D and 3D TEE results, patients were classified as having no shunt, a possible PFO, a definite PFO, or an IPS. If no air bubbles appeared in the LA, the patient was classified into the no-shunt group. The presence of PFO was determined by the appearance of agitated saline bubbles in the left atrium within three cardiac cycles during the Valsalva maneuver, which augments right-to-left shunting by transiently increasing right atrial pressure. PFO grading was based on the number of bubbles (grade 1:  $<10$  bubbles, grade 2: 10–30 bubbles, and grade 3:  $>30$  bubbles)<sup>8</sup>. Since 2D and 3D images are acquired separately and morphological measurements may vary depending on imaging plane and resolution, this grading system was chosen as a consistent and reproducible method that is less affected by such factors and enables standardized comparison across modalities. Definite PFO was diagnosed when the separation of the septum primum and the secundum was visualized with the air bubbles of agitated saline solution passing through it<sup>23</sup>. Possible PFO was defined as meeting the diagnostic criteria for PFO (appearance of air bubbles in the LA within five cardiac beats after opacification of the RA) but does not satisfy the criteria for definite PFO. If air bubbles appeared in LA after three or more cardiac cycles and were observed inside the pulmonary veins moving into the LA, the patient was classified into the IPS group. In patients with PFO confirmed by 3D imaging, the number of bubbles was compared with that in 2D images<sup>24</sup>. Final categorization of shunt type (no shunt, possible PFO, definite PFO, or IPS) was determined by consensus of three experienced echocardiographers after independent review of both 2D and 3D datasets, taking into account septal anatomy, bubble timing, and shunt pathway. Atrial septal aneurysm (ASA) was defined as  $\geq 10$  mm of excursion from the midline<sup>25</sup>. A complex aortic plaque was defined as a plaque that protrudes at least 4 mm into the aortic lumen or a plaque that is associated with ulceration or mobile features<sup>26</sup>. Both 2D cine loops and real-time 3D echocardiographic datasets were stored digitally in raw format and analyzed using the software embedded in TEE (namely, EPIQ CVx).

### Novel 3D protocol for PFO

The most important principle of the novel 3D TEE protocol for PFO detection was that the 3D image should facilitate the demonstration of a PFO en face and demonstrate its relationship with surrounding structures,

including the right atrium, LA, and aorta. Furthermore, to differentiate PFO from IPS, which also exhibits the appearance of air bubbles in the LA, a view demonstrating both the atrial septum and the pulmonic vein may be helpful. The new protocol should not only satisfy the above principles and maximize the advantages of 3D images but also be practical by minimizing the additional effort required of the examiner, the time needed for image acquisition, and the patient's inconvenience. This was considered feasible if the 3D TEE images included the interatrial septum, LA, and pulmonary vein.

Statistical analysis

Continuous variables are presented as means ± standard deviations, and categorical variables are expressed as percentages of the total group. Each 2D and 3D TEE image was evaluated by three blind observers and a single observer at two different time points. The interobserver and intra-observer variabilities in the diagnosis of PFO and IPS were assessed by calculating the k statistics using the Fleiss method<sup>27</sup>.

Results

Baseline characteristics

Table 1 shows the baseline characteristics of the study population. The mean age was 63.6 ± 14.1 years, and 52 patients (34.7%) were female. Among the patients, 112 (74.7%) had hypertension, 57 (38.0%) had diabetes mellitus, 22 (14.7%) had atrial fibrillation, and 93 (59.2%) had dyslipidemia. The etiologies of stroke were ESUS in 127 patients (84.7%), atherosclerosis in 15 patients (10.0%), and lacunar infarction in seven patients (4.7%). The mean NIHSS score was 1.0 (interquartile range: 0.0–3.0), and 23 patients (14.6%) had a history of ischemic stroke. Two-dimensional echocardiography showed LAA thrombus in one patient (0.7%), spontaneous echo contrast in the LAA in five patients (3.3%), ASA in seven patients (4.7%), and complex atheroma in the aortic arch or descending thoracic aorta in 11 patients (7.3%). PFO was diagnosed in 43 patients (28.7%) using 2D TEE, and PFO grades 1, 2, and 3 were observed in 28 (65.1%), 10 (23.3%), and five (11.6%) patients, respectively (Table 2).

Development of a practical 3D TEE protocol for PFO

Figure 1 shows the practical 3D TEE protocol, which consists of two images: one in the 90°–120° degree bicaval view (Fig. 1A and Supplementary Video 1) and another in the 40°–70° degree short-axis view. These images were acquired to include both the left upper pulmonic vein and interatrial septum at the mid-esophageal position (Fig. 1B and Supplementary Video 2). Recordings were initiated at the time of right atrial filling with agitated saline and relief of the Valsalva maneuver and lasted for at least 10 cardiac cycles. The 2D image was converted into a live 3D image using the 3D zoom mode in each view after adjusting the pyramidal datasets to include the IAS, particularly the PFO outlet within the LA side. The 3D images were prospectively stored for a loop length of 20 beats. The recording began when air bubbles filled the right atrium, which was immediately followed by the Valsalva maneuver. Multiple 3D display layouts were used during the recording and simultaneously displayed a 3D volume image and two multiplanar reformation images.

Feasibility of the newly developed 3D protocol

Image acquisition and analysis of the 3D TEE images were feasible in 150 patients (94.9%), and only eight patients had unsuitable 3D images among those who underwent 3D TEE. In the early stages of protocol development, the time required to obtain 3D images according to the protocol was 8.0 ± 3.2 min. However, after passing the learning curve with approximately 20 cases, the time required to obtain 3D images was reduced to 5.5 ± 2.3 min; the patients complained of minor discomfort only. In parallel, the number of agitated saline injections required to complete the protocol also decreased as the operators gained experience.

	N= 150
Age, years	63.6 ± 14.1
Female, n (%)	52 (34.7)
Body mass index, kg/m <sup>2</sup>	25.4 ± 3.3
Hypertension, n (%)	112 (74.7)
Diabetes mellitus, n (%)	57 (38.0)
Dyslipidemia, n (%)	93 (59.2)
Atrial fibrillation, n (%)	22 (14.7)
Smoking, n (%)	41 (27.3)
Etiology of Stroke, n (%)	
ESUS	128 (85.3)
Atherosclerosis	15 (10.0)
Lacunar	7 (4.7)
NIHSS	1.0 (0.0–3.0)
Recurrent ischemic stroke, n (%)	23 (14.6)

**Table 1.** Baseline characteristics of the study population. ESUS, Embolic stroke of Undetermined Source; NIHSS, National. Institute of Health Stroke Scale; 2D, two-dimensional; LAA, left atrial appendage.

	N = 150
2D	
LAA thrombus, n (%)	1 (0.7)
Spontaneous echo contrast in LAA, n (%)	5 (3.3)
LAA emptying velocity, cm/s	70.4 ± 24.5
Complex atheroma, n (%)	11 (7.3)
Atrial septal aneurysm, n (%)	7 (4.7)
2D agitated saline contrast study	
No shunt, n (%)	96 (64.0)
Definite PFO, n (%)	20 (13.3)
Possible PFO, n (%)	23 (15.3)
Intrapulmonary shunt, n (%)	11 (7.4)
Grading of PFO, n (%)	43 (28.7)
Grade 1 (< 10 air bubbles)	28 (65.1)
Grade 2 (10–30 air bubbles)	10 (23.3)
Grade 3 (> 30 air bubbles)	5 (11.6)
3D agitated saline contrast study	
No shunt, n (%)	97 (64.7)
Definite PFO, n (%)	35 (23.3)
Possible PFO, n (%)	5 (3.3)
Intrapulmonary shunt, n (%)	13 (8.7)

**Table 2.** 2D and 3D characteristics of transesophageal echocardiography. LAA, left atrial appendage; 2D, two-dimensional; PFO, patent foramen ovale; 3D, three-dimensional.

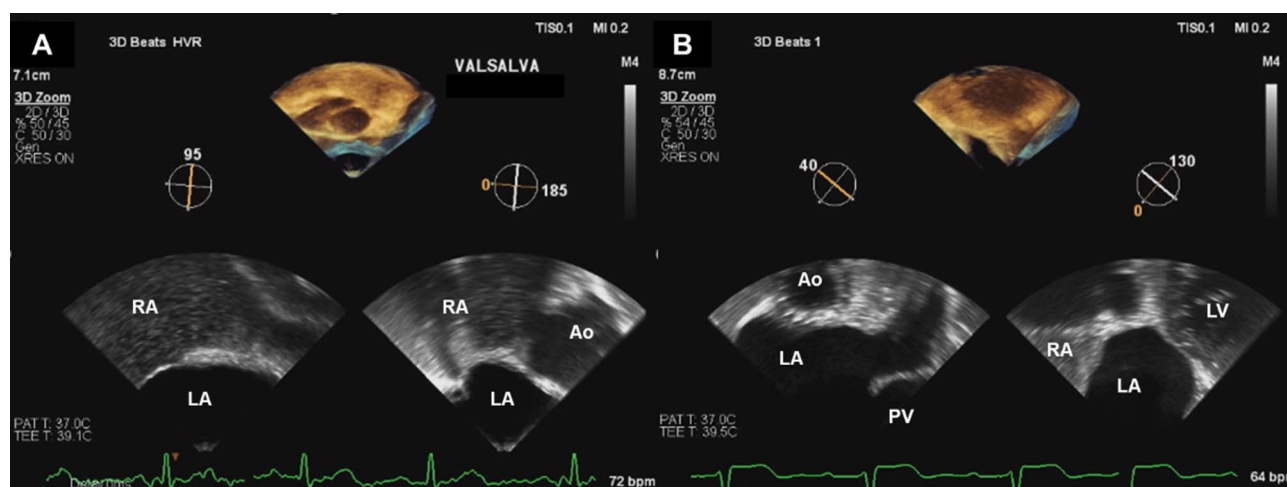


**Fig. 1.** Practical 3D TEE protocol. (A) Mid-esophageal 90°–120° degree bicaval view. (B) Mid-esophageal 40°–70° degree short-axis view.

### Incremental diagnostic value of the newly developed 3D protocol

Among the 150 patients, 2D TEE showed possible PFO in 23 patients (15.3%), definite PFO in 20 patients (13.3%), IPS in 11 patients (7.4%), and no air bubbles in the LA in 96 patients (64.0%).

When 3D TEE images were analyzed for 96 patients in the no-shunt group as categorized using 2D TEE, three patients were identified as having definite PFO, and one patient was identified as having IPS. Among the 23 patients initially judged to have a possible PFO by 2D TEE, only five remained classified as having a possible PFO after applying 3D TEE. A total of 18 patients (78.2%) were reclassified into the other groups: six with no shunt, 13 with a definite PFO (Fig. 2A, Supplementary Videos 3–4), and four with IPS (Fig. 2B, Supplementary Videos 5–6).

Most patients with definite PFO in 2D TEE also had definite PFO in 3D TEE. Eleven cases were judged as IPS in 2D TEE, and seven cases were reclassified as no shunt in 3D TEE. By applying the practical 3D ASC protocol to TEE, 32 patients (21.3%) were reclassified into a different group, and 16 patients (10.7%) had their diagnosis altered. The number of patients classified as having definite PFO increased from 20 (13.3%) to 35 (23.3%) (Fig. 3).

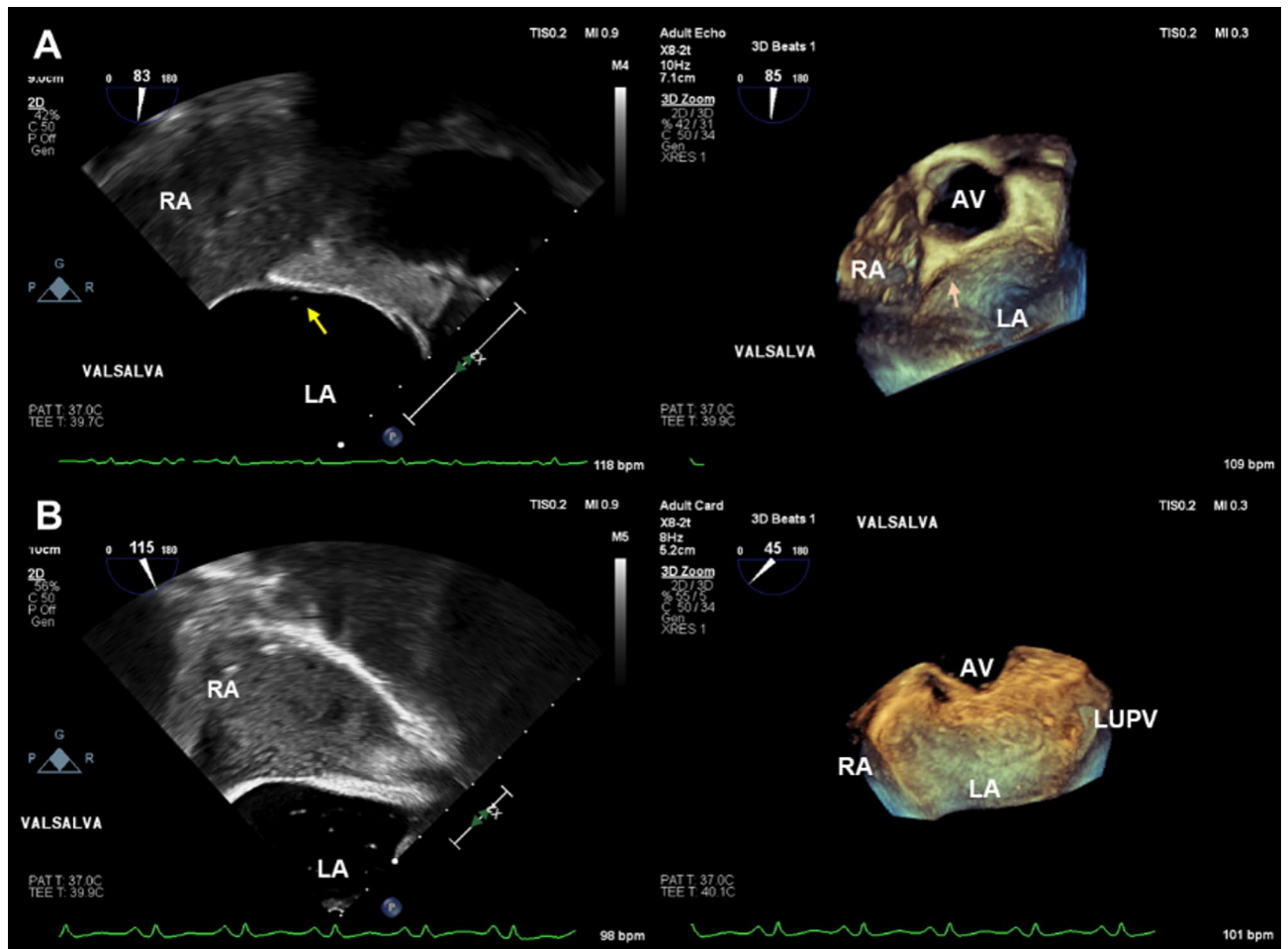


**Fig. 2.** Representative cases. (A) Air bubbles were detected in LA (yellow arrow) without PFO slit separation; possible PFO in 2D TEE, air bubbles were detected in LA with PFO slit separation (orange arrow) observed; definite PFO in 3D TEE. (B) Air bubbles appeared in LA within five cardiac cycles after opacification of RA, without PFO slit separation observed in 2D TEE; possible PFO, and air bubbles coming from the left pulmonic vein; IPS in 3D TEE.

Figure 4 displays the number of air bubbles in the LA in 2D and 3D ASC-TEE in 35 patients diagnosed with definite PFO in 3D TEE. A strong correlation was observed between the number of bubbles in 2D and 3D images ( $r=0.91$ ,  $p<0.001$ ). The number of air bubbles in 3D space was significantly higher than in 2D space because air bubbles are more visible in 3D space ( $9.1 \pm 8.7$  vs.  $15.7 \pm 14.1$ ,  $P=0.013$ ).

#### Interobserver and intra-observer variability

Each observer diagnosed the shunt from 2D and 3D ASC-TEE (Table 3). The overall interobserver k value was 0.83 (0.77–0.89) in the 2D analysis and 0.89 (0.83–0.96) in the 3D analysis. The overall intra-observer k value was 0.83 (0.73–0.92) in the 2D analysis and 0.90 (0.83–0.97) in the 3D analysis (Table 4).

#### Discussion

This study demonstrated the feasibility of a practical protocol for 3D ASC-TEE in the diagnosis of PFO. The 3D TEE allows for direct and simultaneous observation of the interatrial septum and pulmonic vein in 3D space. It can determine the route of air bubbles entering the LA during the ASC test, thus leading to an accurate diagnosis of PFO compared with 2D TEE. Additionally, since only two image acquisitions were performed, patient discomfort and time consumption could be minimized. This study provides a basis for the clinical application of a practical 3D protocol because it is essential to accurately diagnose PFO in patients when evaluating the cardioembolic source of ischemic stroke.

When performing 2D TEE to evaluate a cardiac embolic source, many ambiguous cases are encountered in which a few air bubbles are observed in the LA without the definite separation of the septum primum and secundum or air bubbles coming into the LA from the pulmonary vein. In this study, 23 patients (15.3%) were likely to have a PFO; however, this was not definitively confirmed. Among these patients, 19 had a precise diagnosis of PFO. One patient had no shunt, and five were diagnosed with IPS. Thirteen of the 23 patients were diagnosed with definite PFO, thus adding to the certainty of the diagnosis by 3D TEE. By contrast, almost all



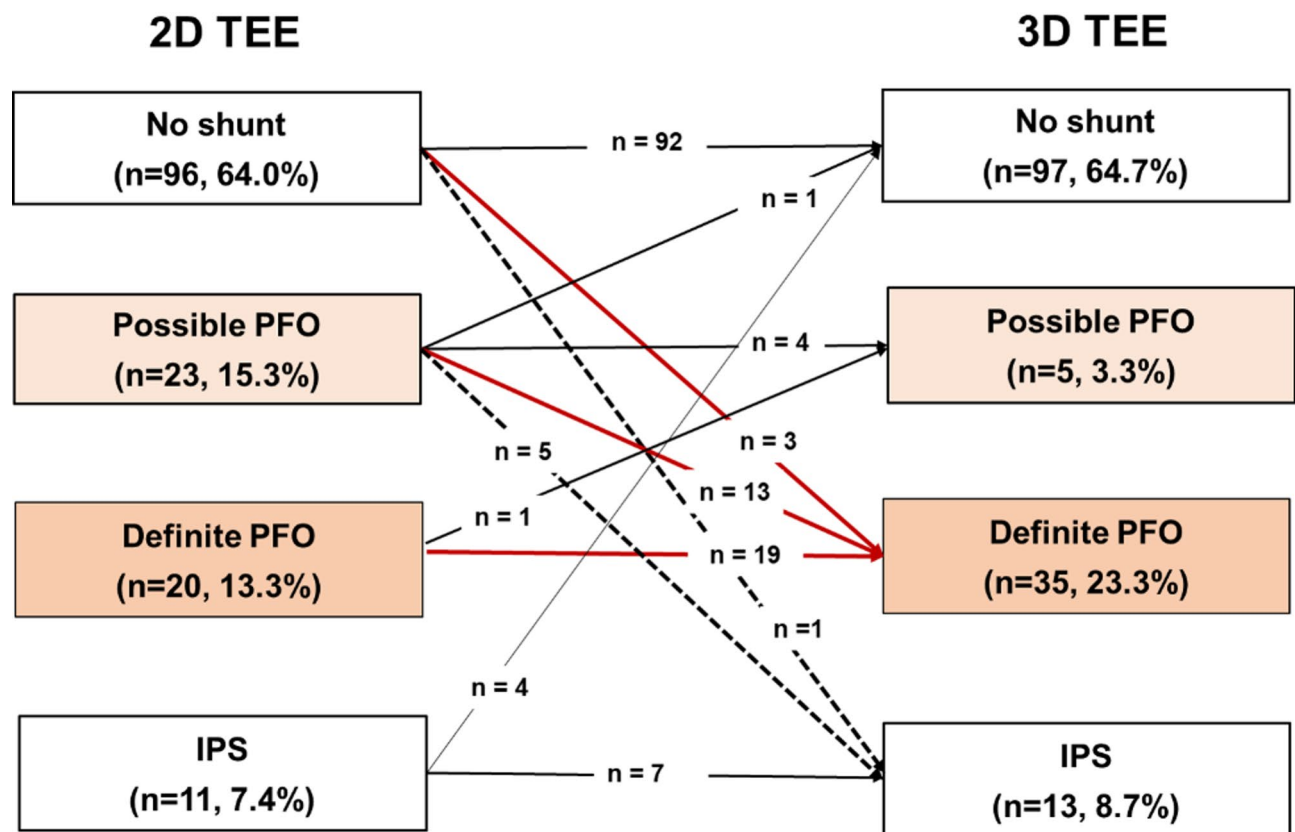


**Fig. 3.** Reclassification of the diagnoses after 3D TEE analysis. By applying the practical 3D ASC protocol to TEE, 32 patients (21.3%) were reclassified into a different group, and 16 patients (10.7%) had their diagnosis altered. The number of patients classified as having definite PFO increased from 20 (13.3%) to 35 (23.3%).

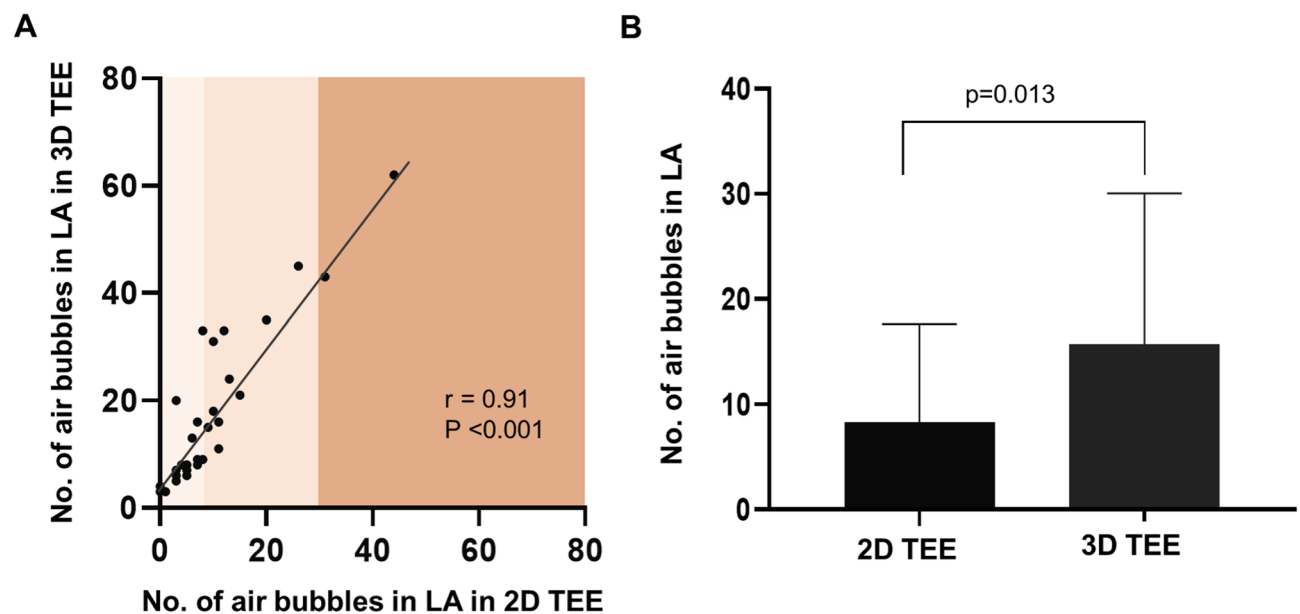


**Fig. 4.** The number of air bubbles in the LA in 2D and 3D ASC-TEE. **(A)** The number of air bubbles in LA in 2D and 3D TEE had a significant correlation ( $r = 0.91$ ,  $p < 0.001$ ). **(B)** The number of air bubbles in 3D space was significantly higher than in 2D space because air bubbles are more visible in 3D space ( $9.1 \pm 8.7$  vs.  $15.7 \pm 14.1$ ,  $P = 0.013$ ).

	Observer		
	1	2	3
2D agitated saline contrast TEE			
No shunt, n (%)	96 (64.0)	86 (57.3)	87 (58.0)
Definite PFO, n (%)	15 (10.0)	20 (13.3)	15 (10.0)
Possible PFO, n (%)	28 (18.7)	24 (16.0)	27 (18.0)
IPS, n (%)	11 (7.3)	20 (13.4)	21 (14.0)
3D agitated saline contrast TEE			
No shunt, n (%)	98 (65.3)	93 (62.0)	95 (63.3)
Definite PFO, n (%)	36 (24.0)	35 (23.3)	33 (22.0)
Possible PFO, n (%)	5 (3.3)	7 (4.7)	7 (4.7)
IPS, n (%)	11 (7.3)	15 (10.0)	15 (10.0)

**Table 3.** Diagnosis of the shunt from 2D and 3D agitated saline contrast TEE by each observer. 2D, two-dimensional; TEE, transesophageal echocardiography; PFO, patent foramen ovale; IPS, intrapulmonary shunt.

	Examiner 1	Examiner 2	Examiner 3
2D			
Examiner 1	0.83 (0.73–0.92)	0.77 (0.69–0.86)	0.84 (0.75–0.93)
Examiner 2			0.74 (0.62–0.85)
Examiner 3			
3D			
Examiner 1	0.90 (0.83–0.97)	0.91 (0.84–0.98)	0.92 (0.86–0.99)
Examiner 2			0.83 (0.73–0.93)
Examiner 3			

**Table 4.** Interobserver and intraobserver variability in the analysis of 2D and 3D TEE images. Overall k statistics for 2D (Fleiss method): 0.83 (0.77–0.89). Overall k statistics for 3D (Fleiss method): 0.89 (0.83–0.96).

patients with a definite PFO in 2D TEE were also confirmed to have a definite PFO in 3D TEE. Thus, it is more helpful in clinical practice to apply the 3D ASC protocol in cases where a definite PFO cannot be diagnosed using 2D TEE.

Real-time 3D TEE provides more detailed information on the interatrial septum than 2D TEE<sup>17,18,21</sup>. Three-dimensional TEE enables the direct localization of the PFO slit opening's separation into the LA and the observation of microbubbles crossing through the PFO, as it provides a live, spatial image. In addition, 3D TEE acquires images of the entire LA space, including the interatrial septum, even when taken only once. Therefore, diagnosis through post-analysis after acquisition is possible, which can reduce examination time and patient discomfort. By contrast, 2D TEE requires multiple images to be acquired to make a diagnosis. Therefore, patients with an ambiguous diagnosis from 2D TEE may be more accurately diagnosed by adding the 3D TEE technique, which provides a comprehensive observation of the entire atrial septum and adjacent structures.

However, there are a few drawbacks to 3D TEE images. First, the image quality depends on the examiner's skill and ability to perform proper Valsalva maneuvers. Second, a 3D image has a lower temporal resolution than a 2D image. The narrowing of the acquisition sector or multiple-beat acquisitions, typically used to improve temporal resolution, is challenging to apply to dynamically fluttering structures.

No standard exists for grading the severity of PFO based on the results of 3D TEE. In this study, the number of air bubbles visualized in the 3D space of the LA was higher than that in the 2D space. This indicates that modality-specific criteria may be necessary. Larger multicenter studies are warranted to validate and refine these thresholds in the future. Furthermore, future perspectives for diagnosing PFO using 3D TEE include applying color-coded air bubbles for easier tracking and employing artificial intelligence to accurately count the number and timing of air bubbles. If there are more advantages to 3D than 2D when applying new technology, the time for PFO diagnosis can be shortened by using only 3D instead of 2D in the future<sup>28</sup>.

This study had several limitations. First, this was a single-center study that was conducted using TEE equipment from a specific vendor. TEE was conducted by physicians familiar with 3D echocardiography using advanced TEE probes and machines; therefore, it will be challenging to apply our results to different situations. Second, there is no gold standard for determining which 2D and 3D results are the most accurate. However, the results of some cases of PFO occlusion or CT pulmonary angiogram revealed that a 3D image could provide a more precise diagnosis than a 2D image. Third, there are still cases in which the diagnosis is unclear even after applying the 3D protocol. Fourth, although sufficient time was allowed between injections to minimize residual microbubbles, we cannot entirely exclude the possibility that late-arriving bubbles may have confounded the interpretation in some cases. Fifth, Bacteriostatic saline, which may improve bubble yield, is not commercially available in Korea, and therefore, preservative-free sterile saline was used. In addition, the

final diagnostic classification was made through expert consensus rather than based on a universally accepted reference standard, which may introduce a degree of subjectivity despite efforts to standardize interpretation using predefined criteria.

## Conclusion

The 3D ASC-TEE protocol developed for the diagnosis of PFO is practical and feasible (94.9%) in patients with ischemic stroke. Three-dimensional TEE would be helpful for the accurate diagnosis of PFO, not only in structural evaluation but also in functional evaluation in the era of transcatheter PFO closure. Therefore, this practical 3D TEE protocol for PFO could be applied as a routine clinical procedure for evaluating the cardiac source of embolism.

## Data availability

The data that support the findings of this study are available on request from the corresponding author.

Received: 5 November 2024; Accepted: 4 August 2025

Published online: 09 August 2025

## References

- Mas, J. L. et al. Patent foramen ovale and atrial septal aneurysm study group. Recurrent cerebrovascular events associated with patent foramen ovale, atrial septal aneurysm, or both. *N Engl. J. Med.* **345** (24), 1740–1746 (2001).
- Baik, M. et al. Patent foramen ovale and risk of recurrence in stroke of determined etiology. *Ann. Neurol.* **92** (4), 596–606 (2022).
- Ntaios, G. Embolic stroke of undetermined source: JACC review topic of the week. *J. Am. Coll. Cardiol.* **75** (3), 333–340 (2020).
- Lee, P. H. et al. Cryptogenic stroke and High-Risk patent foramen ovale: the DEFENSE-PFO trial. *J. Am. Coll. Cardiol.* **71** (20), 2335–2342 (2018).
- Schuchlenz, H. W. et al. Transesophageal echocardiography for quantifying size of patent foramen ovale in patients with cryptogenic cerebrovascular events. *Stroke* **33** (1), 293–296 (2002).
- Kent, D. M. et al. Heterogeneity of treatment effects in an analysis of pooled individual patient data from randomized trials of device closure of patent foramen ovale after stroke. *JAMA* **326** (22), 2277–2286 (2021).
- Silvestry, F. E. et al. American society of echocardiography; society for cardiac angiography and interventions. Guidelines for the echocardiographic assessment of atrial septal defect and patent foramen ovale: from the American society of echocardiography and society for cardiac angiography and interventions. *J. Am. Soc. Echocardiogr.* **28** (8), 910–958 (2015).
- Bernard, S., Churchill, T. W., Namasivayam, M. & Bertrand, P. B. Agitated Saline Contrast Echocardiography in the Identification of Intra- and Extracardiac Shunts: Connecting the Dots. *J. Am. Soc. Echocardiogr.* S0894-7317(20)30615-5 (2020).
- Song, J. K. Pearls and pitfalls in the transesophageal echocardiographic diagnosis of patent foramen ovale. *J. Am. Soc. Echocardiogr.* **36** (9), 895–905e3 (2023).
- D'Andrea, A. et al. EACVI survey on the management of patients with patent foramen ovale and cryptogenic stroke. *Eur. Heart J. Cardiovasc. Imaging* **22** (2), 135–141 (2021).
- Bhatia, N., Abushora, M. Y., Donneyong, M. M. & Stoddard, M. F. Determination of the optimum number of cardiac cycles to differentiate intra-pulmonary shunt and patent foramen ovale by saline contrast two- and three-dimensional echocardiography. *Echocardiography* **31** (3), 293–301 (2014).
- Freeman, J. A. & Woods, T. D. Use of saline contrast echo timing to distinguish intracardiac and extracardiac shunts: failure of the 3- to 5-beat rule. *Echocardiography* **25** (10), 1127–1130 (2008).
- Woods, T. D. & Patel, A. A critical review of patent foramen ovale detection using saline contrast echocardiography: when bubbles lie. *J. Am. Soc. Echocardiogr.* **19** (2), 215–222 (2006).
- Kim, I. C. et al. Comparison of cardiac computed tomography with transesophageal echocardiography for identifying vegetation and intracardiac complications in patients with infective endocarditis in the era of 3-Dimensional images. *Circ. Cardiovasc. Imaging* **11** (3), e006986 (2018).
- Perk, G. et al. Use of real time three-dimensional transesophageal echocardiography in intracardiac catheter based interventions. *J. Am. Soc. Echocardiogr.* **22** (8), 865–882 (2009).
- Lang, R. M. et al. American society of echocardiography; European association of echocardiography. EAE/ASE recommendations for image acquisition and display using three-dimensional echocardiography. *J. Am. Soc. Echocardiogr.* **25** (1), 3–46 (2012).
- Saric, M., Perk, G., Purgess, J. R. & Kronzon, I. Imaging atrial septal defects by real-time three-dimensional transesophageal echocardiography: step-by-step approach. *J. Am. Soc. Echocardiogr.* **23** (11), 1128–1135 (2010).
- Shanks, M. et al. Detection of patent foramen ovale by 3D echocardiography. *JACC Cardiovasc. Imaging* **5** (3), 329–331 (2012).
- Hart, R. G., Catanese, L., Perera, K. S., Ntaios, G. & Connolly, S. J. Embolic stroke of undetermined source: A systematic review and clinical update. *Stroke* **48** (4), 867–872 (2017).
- Johansson, M. C., Eriksson, P., Guron, C. W. & Dellborg, M. Pitfalls in diagnosing PFO: characteristics of false-negative contrast injections during transesophageal echocardiography in patients with patent foramen ovals. *J. Am. Soc. Echocardiogr.* **23** (11), 1136–1142 (2010).
- Saric, M. et al. Guidelines for the use of echocardiography in the evaluation of a cardiac source of embolism. *J. Am. Soc. Echocardiogr.* **29** (1), 1–42 (2016).
- Porter, T. R. et al. Guidelines for the cardiac sonographer in the performance of contrast echocardiography: a focused update from the American society of echocardiography. *J. Am. Soc. Echocardiogr.* **27** (8), 797–810 (2014).
- Lee, J. Y. et al. Association between anatomic features of atrial septal abnormalities obtained by omni-plane transesophageal echocardiography and stroke recurrence in cryptogenic stroke patients with patent foramen ovale. *Am. J. Cardiol.* **106** (1), 129–134 (2010).
- Tanaka, J. et al. Comparison of two-dimensional versus real-time three-dimensional transesophageal echocardiography for evaluation of patent foramen ovale morphology. *Am. J. Cardiol.* **111** (7), 1052–1056 (2013).
- Mügge, A. et al. Atrial septal aneurysm in adult patients. A multicenter study using transthoracic and transesophageal echocardiography. *Circulation* **91** (11), 2785–2792 (1995).
- Di Tullio, M. R. et al. Aortic atheromas and acute ischemic stroke: a transesophageal echocardiographic study in an ethnically mixed population. *Neurology* **46** (6), 1560–1566 (1996).
- Cabanes, L. et al. Patent foramen ovale and atrial septal aneurysm study group. Interobserver and intraobserver variability in detection of patent foramen ovale and atrial septal aneurysm with transesophageal echocardiography. *J. Am. Soc. Echocardiogr.* **15** (5), 441–446 (2002).
- Rong, L. Q. An update on intraoperative three-dimensional transesophageal echocardiography. *J. Thorac. Dis.* **9** (Suppl 4), S271–S282 (2017).



## Acknowledgements

We would like to express sincere gratitude to Hee Jeong Lee, Kyung Eun Ha, and Kyu-Yong Ko for their invaluable assistance in acquiring the echocardiographic images.

## Author contributions

SG and CS conceptualized this study. The data curation was carried out by SG, KK, HL, IC, and GH. Investigation efforts were made by SG and KK. The methodology was developed by SG, IC, JH, and CS. The project supervision was provided by CS. The original draft was written by SG. The review and editing were done by SG and CS. All authors read and approved the final manuscript.

## Funding

This work was supported by a grant from the Korea Health Technology R&D Project via the Korea Health Industry Development Institute funded by the Ministry of Health and Welfare, Republic of Korea (grant number: HI22C0154). The funders played no role in the design of the study; collection, analysis, or interpretation of data; writing of the manuscript; or decision to publish the results.

## Declarations

### Ethics approval and consent to participate

The study was approved by the Institutional Review Board of Yonsei University Health System (IRB number: 4-2023-0318) and was conducted in accordance with the Declaration of Helsinki. Informed consent was waived for this study as approved by the Institutional Review Board of Yonsei University Health System in accordance with applicable guidelines and regulations.

### Competing interests

The authors declare no competing interests.

### Additional information

**Supplementary Information** The online version contains supplementary material available at <https://doi.org/10.1038/s41598-025-14873-5>.

**Correspondence** and requests for materials should be addressed to C.Y.S.

**Reprints and permissions information** is available at [www.nature.com/reprints](http://www.nature.com/reprints).

**Publisher's note** Springer Nature remains neutral with regard to jurisdictional claims in published maps and institutional affiliations.

**Open Access** This article is licensed under a Creative Commons Attribution-NonCommercial-NoDerivatives 4.0 International License, which permits any non-commercial use, sharing, distribution and reproduction in any medium or format, as long as you give appropriate credit to the original author(s) and the source, provide a link to the Creative Commons licence, and indicate if you modified the licensed material. You do not have permission under this licence to share adapted material derived from this article or parts of it. The images or other third party material in this article are included in the article's Creative Commons licence, unless indicated otherwise in a credit line to the material. If material is not included in the article's Creative Commons licence and your intended use is not permitted by statutory regulation or exceeds the permitted use, you will need to obtain permission directly from the copyright holder. To view a copy of this licence, visit <http://creativecommons.org/licenses/by-nc-nd/4.0/>.

© The Author(s) 2025